Hybrid Moth-Flame Fuzzy Logic Controller Based Integrated Cuk Converter Fed Brushless DC Motor for Power Factor Correction

K. Kamalapathi [1], Neeraj Priyadarshi [2,*], Sanjeevikumar Padmanaban [3,*], Farooque Azam [4,*] , C. Umayal [5], Vigna K. Ramachandaramurthy [6]

[1,5]School of Electrical Engineering, VIT University- 600127, India; kamal.kuditi@gmail.com (K.K), umayal.c@vit.ac.in (C.U).
[2]Department of Electrical Engineering, Birsa Institute of Technology (Trust), Ranchi- 835217, India; neerajrjd@gmail.com (N.P.).
[3] Department of Energy Technology, Aalborg University, 6700 Esbjerg, Denmark
[4] School of Computing & Information Technology, REVA University, Bangalore, 560064, India; farooque53786@gmail.com (F.A.)
[6] Institute of Power Engineering, Department of Electrical Power Engineering, Universiti Tenaga Nasional,Kajang 43000, Malaysia; vigna@uniten.edu.my (V.K.R.)
* Correspondence: neerajrjd@gmail.com (N.P.)

Abstract- This research work deals hybrid control system based integrated Cuk converter fed brushless DC motor (BLDCM) for power factor correction. In this work, moth-flame optimization (MFO) and fuzzy logic controller (FLC) has been combined and moth –flame fuzzy logic controller (MFOFLC) has been proposed. Firstly, the BLDC motor modelling is composed with power factor correction (PFC) based integrated Cuk converter and BLDC speed is regulated using variable DC-Link inverter voltage which makes low switching operation with less switched losses. Here, with the use of switched inductor, the task and execution of proposed converter is redesigned. The DBR (diode bridge rectifier) trailed by proposed PFC based integrated Cuk converter operates in discontinuous inductor conduction mode(DICM) for achievement of better power factor.MFO is exhibited for gathering of dataset from the input voltage signal. At that point separated datasets is send to FLC to improve the updating function and minimization of torque ripple. However, our main objective is to assess adequacy of proposed method, the power factor is broke down. The execution of the proposed control methodology is executed in MATLAB/Simulink working platform and the display is assessed with the existing techniques.

Keywords: BLDC (brushless DC) motor; VSI, Fuzzy logic controller; Moth flame optimization;Torque ripples.

1. Introduction

Nowadays a trend to use Brushless DC motor rather than brushed DC motor in an expanding number of uses [1]. Compared to brush DC motors and induction motors, BLDC motor has a couple of favourable circumstances [2]. It works as a synchronous motor in which stator and rotor magnetic field generates comparative frequency. BLDC engines don't encounter the "slip" that is consistently found in induction motors [3]. Regularly, the BLDCM is made out of three stator coils with a permanent magnetic rotor in which magnetic field is turned by 2 coils and floating coil is responsible for back EMF.[4]. Speed regulation is a fundamental viewpoint as far as BLDC speed and position controlling is concerned [5-7].

As an average speed controller framework, it employed double-loop structure which can be used in multiple applications like in household; electronics based self-propelled, précised apparatus and automated systems used in offices, and so forth [8].

Because of torque ripple commutation, BLDC motor has torque ripple problem.. Subsequently, concealment of torque ripplecommutation is responsible for reduction of torque ripple in BLDC motor[9]. The torque for the most part incorporates cogging, mutual, andreluctance torque.Cogging torque has been activated using stator connected rotor's magnetic field which is independent from stator's current excitation [10, 11]. Because of power electronic commutation, torque ripples are generated which is responsible for highswitched frequency and stator's blemish [12]. The trapezoidal back-EMF is responsible for reduction of torque ripples in BLDC motor which can be achieved by utilizing condensed winding and use of one pitch slot with skewed stator slot skewing [13, 14]. Therefore a productive controller is required for minimization of supply voltage and line current harmonics present in motor system [15].

Practically speaking, the design of the BLDC motor drive includes a mind boggling procedure.Traditionally, various BLDC motor speed controller have been discussed in literature [16]. Phase change method, hysteresis current method, pulse width modulation (PWM) controller have already been discussed to smoothen torque ripple in BLDC motor but unable to handle over or under compensation problems [17]. Sensors are employed for rotor speed and position estimations [18]. Proportional Integral (PI) based speed controller has been used for this purpose but has more rise/settled time with high speed oscillations are the major issues [19]. Routinely, least-squares approximation strategy, genetic algorithm (GA), particle swarm optimization (PSO) algorithm, NN (neural network) and enhanced gradient descent algorithm has been discussed to improve speed and positions estimation of BLDC motor [20, 21].

Now a day, regulation of speed and torque with torque ripple minimization is a great concern of BLDX motor. PWM controllers are the best suited technology for controlling BLDC motor in which two-phase feeding scheme has been employed. However, it has vulnerability issue because of load as well as in set speed variations. Additionally, tuning of the PID controller prompts vulnerability in the control system parameters. To overcome these challenges, optimal torque control technique utilizing advanced technology is required. Here, an enhanced controller has been employed which solves above issues. MFO technique, numerous parameters will be considered which will identify with the PFC and torque ripple minimization, for example, the speed, torque, back EMF, torque ripple and so forth individually.Using these parameters, the objective function will be characterized that will be comprehended by the MFO strategy.Simulation results reveal employed controller exhibit and predicts best control signals to the converter. The accompanying section portrays the configuration of the proposed converter.

Whatever is left of this paper is sorted out as takes after: In area 2, the current research work is examined. The design and modelling of proposed converter and BLDC motor is indicated in area 3. The proposed control algorithm is portrayed in area 4. The itemized examination and re-enactment after-effect of the proposed method is displayed in segment 5. At long last, segment 6 finishes up the paper.

Preprints (www.preprints.org) | NOT PEER-REVIEWED | Posted: 24 September 2018 doi:10.20944/preprints201809.0462.v1

Peer-reviewed version available at *Electronics* **2018**, *7*, 288; doi:10.3390/electronics7110288

2. PFC of BLDC Motor utilizing Proposed Technique

The schematic of proposed BLDC motor correcting power factor scheme with controlling strategy is appeared in Figure 1. Here, the BLDC motor comprises of two phase: modelling and controlling phases. This framework constitutes an AC voltage as input source, voltage source inverter, integrated Cuk converter, MFFLC based controller as main components. In modelling phase, the BLDC motor is associated with three phases of voltage source inverter (VSI). After thatwith respect to neutral point (N) the phase voltage is estimated.IGBT are employed for inverter lower frequency execution. In controlling phase, a MFFLC strategy is applied for efficiency enhancement of DC motor through switched inductor operation. Also, BLDC electronic commutation and speed regulation is carried out with PWM pulses to the inverter. Generally, the VSI comprises of six solid-state switches which encounters more switched losses because of higher PWM pulses used in motor speed control.The following sections elaborate proposed system design, BLDC motor modelling and control methodologies.

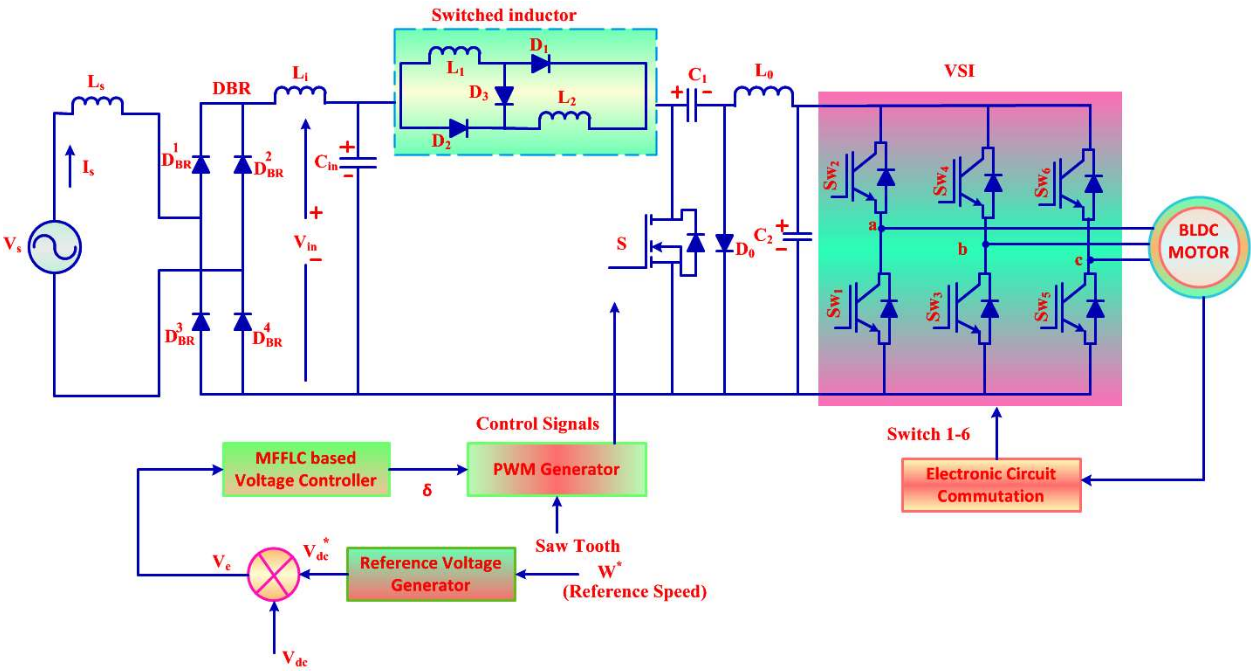

Figure 1. Schematic structure of integrated Cuk converter based controlling strategy for BLDCM

2.1. Modelling Phase

The design of Cuk converter and modelling of BLDC motor is described in this section. Initially, the three phase (AC) supply is given as input source to DBR which is defined in equation (1).

$$V_S(t) = V_m \times \sin(\omega t) \quad (1)$$

Where, $\omega = 2\pi \times f$

f is line frequency and V_m represents peak input voltage

Preprints (www.preprints.org) | NOT PEER-REVIEWED | Posted: 24 September 2018 doi:10.20944/preprints201809.0462.v1

Peer-reviewed version available at *Electronics* **2018**, *7*, 288; doi:10.3390/electronics7110288

The voltage appearing after DBR is

$$V_i(t) = |V_m \times \sin(\omega t)| \qquad (2)$$

The DBR is utilized for converting the input AC voltage to DC voltage and the direct current supply is given to switched inductor.Voltage/current stress occurs while giving DC supply in boost segment and power factor corrected based power switch is expanded in DICM (discontinuous inductor current mode).Consequently, the Cuk converter works as a inverter is [22] which consists of a switch, diode, switched inductors and capacitors. Inductor gets parallel charged in case of switch ON condition and discharge in series during OFF condition with same energy level. Here, the switched inductors have beenmainlyutilizedfor transferring supply and output voltages to current source [23, 24]. The following section includes the design and performance of proposed converter with different modes.

2.1.1 Design of Integrated Converter with VariousModes

Integrated Cuk converter operates in various modes of Continuous Conduction Mode and discontinuous conduction mode. DICM (Discontinuous Inductor Current Mode) and Discontinuous Capacitor Voltage Mode (DCVM) are treated as two modes of discontinuous conduction mode operation. The Cuk converter execution [25] in CCM is described as following intervals. In the first interval, when switch S is turn ON, the switched L_1 and L_2 store energy while C_1 discharge energy which is shown in Figure 2 (a). In the second interval, the S is turned OFF , the switched inductor is responsible for energy storing and C_1gets discharged using switch (S) which relocates DC link capacitor (C_2) depicted with Figure 2 (b).

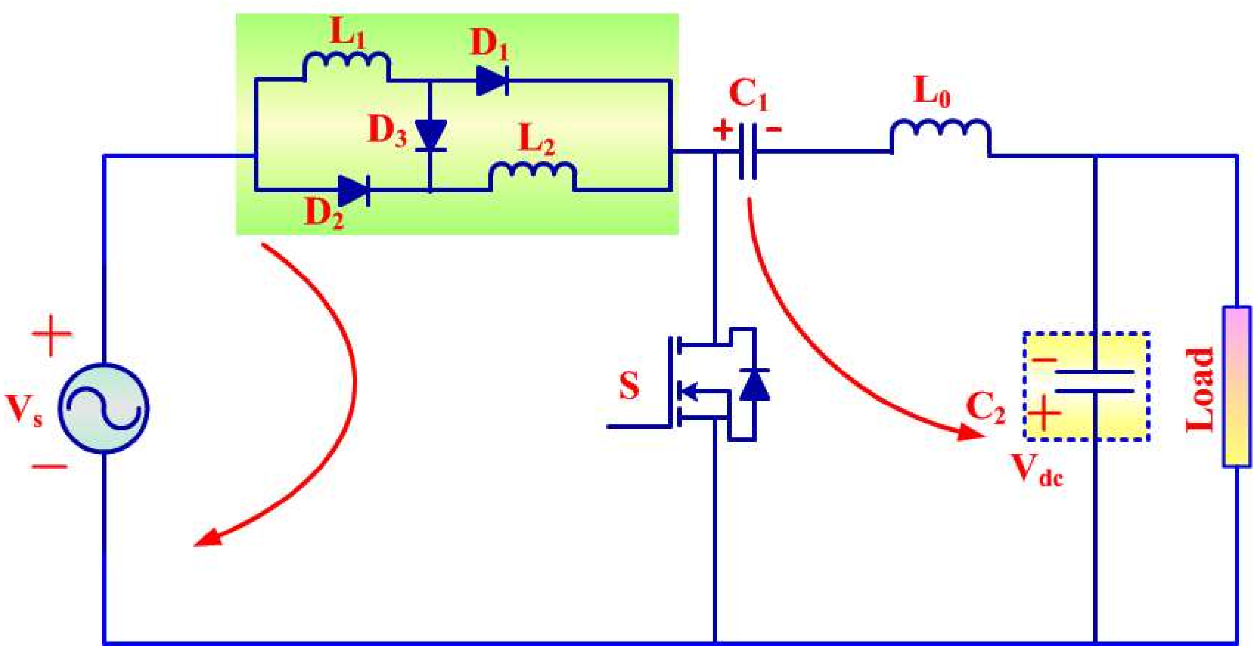

(a)

Preprints (www.preprints.org) | NOT PEER-REVIEWED | Posted: 24 September 2018 doi:10.20944/preprints201809.0462.v1

Peer-reviewed version available at *Electronics* **2018**, *7*, 288; doi:10.3390/electronics7110288

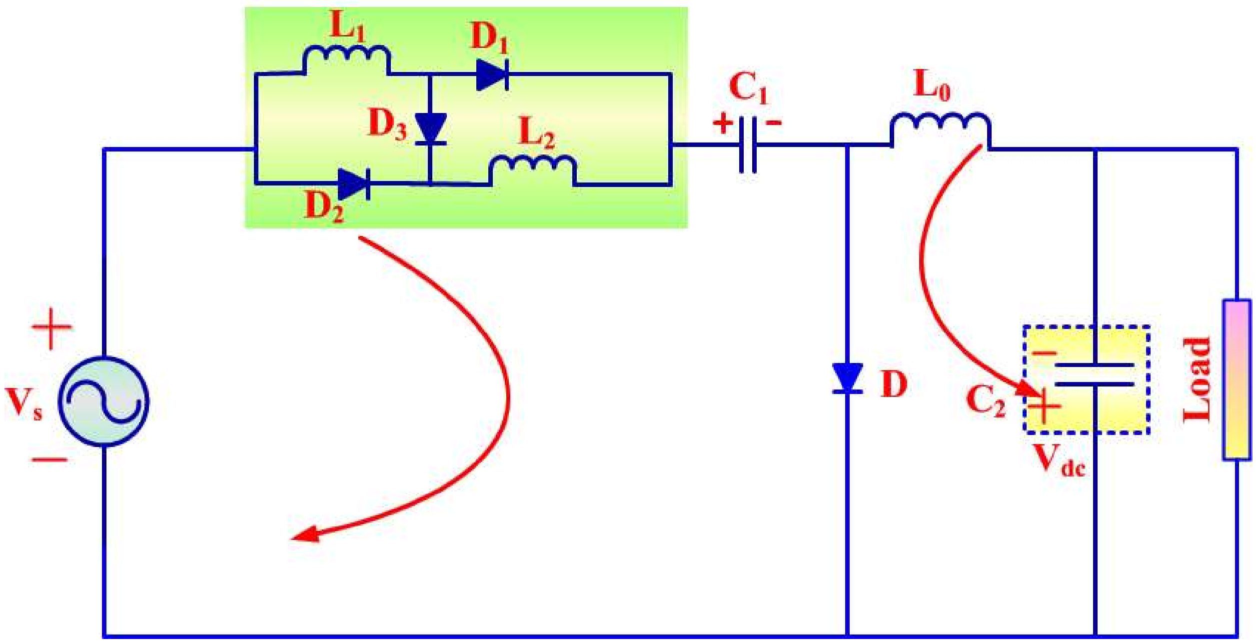

(b)

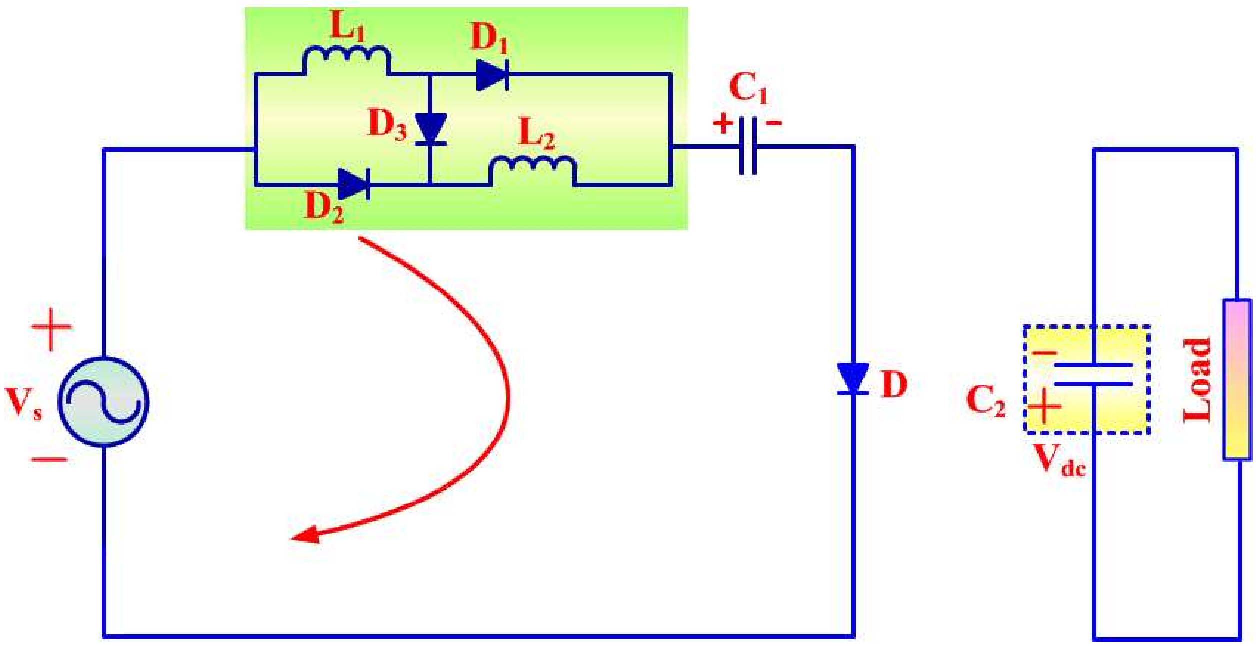

(c)

Peer-reviewed version available at Electronics 2018, 7, 288; doi:10.3390/electronics7110288

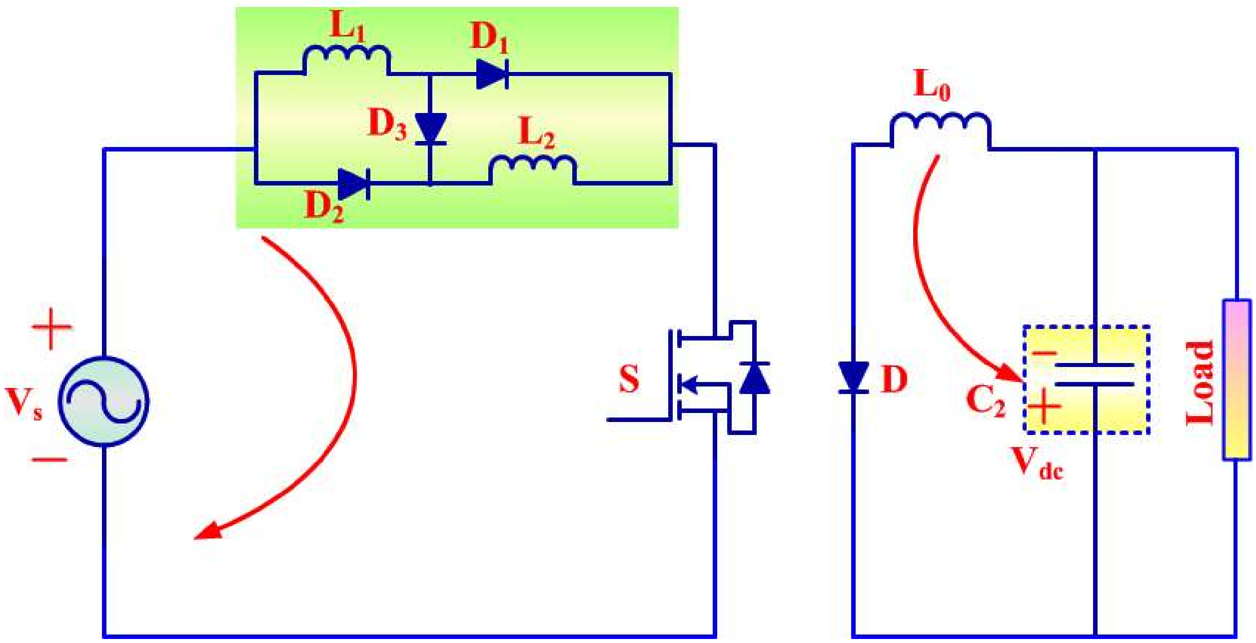

(d)

Figure 2. Design of integrated Cuk converter with different intervals of switching period:(a, b) CCM mode, (c)DICM and (d) DCVM modes

The operation of integrated Cuk converter in DICM and DCVM [26] operation with different intervals of switching period is illustrated using Figure 2 (c) and (d). In first interval, S works in conduction state, the inductor stores energy and discharged in capacitor through switch and energy transferring to C_2.While S gets OFF in second state but C_1 (intermediate capacitor) completely discharged energy and performs DCM operation; hence no energy is left in switched inductor input and voltage remains zero during this operation. In third interval, the intermediate capacitor starts charging continuously by input inductor L_1 during turn off condition.

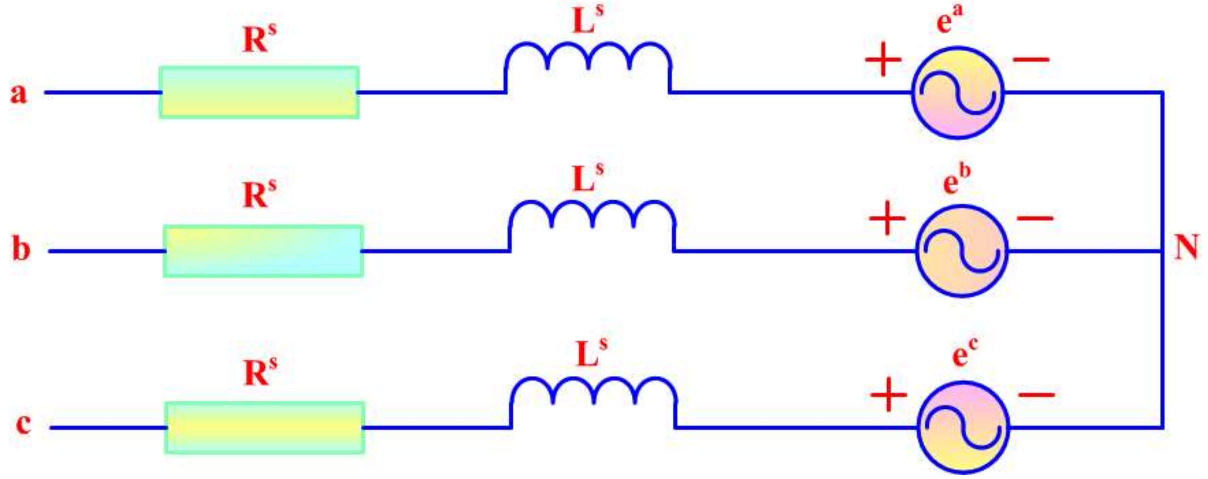

Figure 3. BLDCM- Equivalent model

Preprints (www.preprints.org) | NOT PEER-REVIEWED | Posted: 24 September 2018 doi:10.20944/preprints201809.0462.v1

Peer-reviewed version available at Electronics 2018, 7, 288; doi:10.3390/electronics7110288

Then the output summed energy is given to VSI, so that the voltage level is increased. Then, the VSI is connected to the BLDC motor [27] for controlling speed and torque. Figure 3 illustrates the equivalent circuit of motor phase.

Voltage condition of BLDCM is composed of following equation (3).

$$\Delta^{s}_{abc} = \frac{d}{dt}.\left(F^{s}_{abc}\right) + R^{s} \times .I^{s}_{abc} \qquad (3)$$

Where, r^{s} represents stator resistance, stator voltage is Δ, I is stator current and F denotes flux linkage. Stator's resistance matrix can be calculated in following condition (4).

$$r^{s} = diagonal\left[r^{s}, r^{s}, r^{s}\right] (4)$$

The electromagnetic torque τ^{e} is created by considering back-EMF is characterized as

$$\tau^{e} = \sum_{N=`1}^{\infty} (2N-1).K_{2N-1}.\begin{bmatrix} I^{s}_{a} \\ I^{s}_{b} \\ I^{s}_{c} \end{bmatrix}.(pF^{1}_{m}/2).\begin{bmatrix} \cos\left(\theta^{r}.(2N-1)\right) \\ \cos\left((2N-1).\left(\theta^{r} - \frac{2x}{3}\right)\right) \\ \cos\left((2N-1).\left(\theta^{r} + \frac{2x}{3}\right)\right) \end{bmatrix}. (5)$$

Evaluation of phase back-EMF voltages at the stator terminalsis carried out by rotating the machine with prime mover and open circuit terminal. The mechanical condition of motor speed is expressed as

$$\frac{d}{dt}.\left(\chi^{\gamma}\right) = \left(\frac{P}{2j}\right).\left(\tau^{e} - \tau^{m}\right) \qquad (6)$$

Here, $\frac{d}{dt}.\left(\chi^{\gamma}\right)$is the rotor angular speed with respect to t, p represents magnetic poles number and τ^{m} specify mechanical torque. In the proposed method the normal and speed reference is estimated from the speed estimator and the torque ripple of BLDC motor are minimized from the control strategy is specified in the below section.

2.2 Controlling Phase

Speed /Torque of BLDCM has been controlled using proposed method based PI (proportional integral) controller is developed. From Figure 1, the output signals from VSI generated the optimal pulses, for controlling motor.

(a) VoltageController

Preprints (www.preprints.org) | NOT PEER-REVIEWED | Posted: 24 September 2018 doi:10.20944/preprints201809.0462.v1

Peer-reviewed version available at Electronics 2018, 7, 288; doi:10.3390/electronics7110288

The PI is the feedback control loop mechanism used in control system. Here, the BLDC motor speed is estimated by utilizing the speed estimator. From actual and reference value the speed error is calculated and passed through voltage controller for speed controlling and error correcting. The output of PI controller depends on K_i and K_p parameters and is specified as

$$I = K_p \times e_s(t) + K_i \times e_s(t) \quad (7)$$

In general, the proportional gain (K_p) is providing the entirecontrollingperformance. It can be expressed as proportional to signal error with associated gain and the transfer function is given as follows.

$$I = K_p^{best} \times e_s(t) + K_i^{best} \times \int dt).e_s(t) \quad (8)$$

Where, $e_s(t) = V_{dc} - V_{dc}^{*}$

In the proposed controller, by utilizing the FLC method, MFO strategy is executed and updated. Hence, the gain parameters value (K_p^{best}) is stored from the output of the proposed controller algorithm. Thus, the optimal value of poweris controlled and the controlled signal is given to PWM generator for controlling inverter switching operation and BLDC motor performance. The torque ripples is minimized from the following equation (9).

$$\tau_{ripple} = \frac{t_{\max} - t_{\min}}{t_{\max} + t_{\min}} \quad (9)$$

For generating the optimal control pulses of motor the torque is applied as input for the proposed method by multiplying with 100 and evaluated the torque ripple percentage. The developed mathematical equation for optimal control signals is formulated as

$$DC(t) = if \begin{cases} e(t) > TH; & DC(t) = t_{on} \\ e(t) < TH; & DC(t) = t_{off} \end{cases} \quad (10)$$

Here, TH is the threshold value, t_{on} is on and t_{off} off period of the switches and the duty cycle is represented as $DC(t)$. With the Figure 1 the modelling of BLDC motor is composed.The following section explained the detailed working procedures of proposed MFFLC control approach for getting optimal pulses.

3. Proposed MFFLC Algorithm

MFO method is basically based on transverse direction of moths in universe which works on navigation methodology [28-30]. The MFFLC method will be the joined execution of both MFO and FLC for controlling the motor speed and torque of BLDC motor. The MFO can have the capacity to enhance the

Preprints (www.preprints.org) | NOT PEER-REVIEWED | Posted: 24 September 2018 doi:10.20944/preprints201809.0462.v1

Peer-reviewed version available at *Electronics* **2018**, *7*, 288; doi:10.3390/electronics7110288

underlying irregular arrangements and joining to a superior point in the pursuit space.Here, MFO method can be employed to differentiate proper and accessible required orientation with the selection of suitable activation function. In light of fulfilled dataset, the FLC performs and predicts the most ideal control signals of the converter.With this control strategy, the BLDC motor speed and PFC will be regulated; likewise the harmonicsand torque ripples will be minimized.The MFO algorithm consists of following steps.

3.1. Steps for Proposed MFO Algorithm

Step 1: Setting of Parameters

Voltage, currentand speed variables are the deciding parameters. Number of *dim* variables, $Max\_iteration$,moths and flames numbers, and lower bound (lb) and upper bound (ub) of variables is defined as $lb=[lb_1,lb_2,.........,lb_{n-1},lb_n]$ and $ub=[ub_1,ub_2,.........,ub_{n-1},ub_n]$ are considered as MFO main parameters.

Step 2: Initialization

In MFO algorithm the moths arrangement is initialized in aform of matrix, since it is a population based algorithm.

$$A_M=\begin{bmatrix} A_{1,1} & A_{1,2} & R\,R & A_{1,m} \\ A_{2,1} & A_{2,2} & R\,R & A_{1,m} \\ M & M & M\,M & M \\ A_{n,1} & A_{n,2} & R\,R & A_{n,m} \end{bmatrix} \quad (11)$$

Where, the matrix location of moths is A_M, $A_{i,j}$ is the j^{th} parameter (variables) value of the moth (i^{th}) , $i=1,2,R,n.$ and $j=1,2,R,m$. By using the random distribution $A_{i,j}$ can be given as in equation (12).

$$A_M(i,j)=(upperbound(i)-lowerbound(i))*rand+lowerbound(i) \quad (12)$$

Here, $rand$ denotes uniform randomly created values lies in [0, 1].Theset of flames are expressed as:

$$B=\begin{bmatrix} b_{1,1} & b_{1,2} & K & K & b_{1,m} \\ b_{2,1} & b_{2,2} & K & K & b_{1,m} \\ M & M & M & M & M \\ b_{n,1} & b_{n,2} & K & K & b_{n,m} \end{bmatrix} \quad (13)$$

Where, the matrix location of flames is B, $b_{i,j}$ represents the j^{th} parameter value of i^{th} flame, $i=1,2,K,n.$ and $j=1,2,K,m$. FLC values are randomly initiated with iterations $i=i+1$.

Preprints (www.preprints.org) | NOT PEER-REVIEWED | Posted: 24 September 2018 doi:10.20944/preprints201809.0462.v1

Peer-reviewed version available at Electronics 2018, 7, 288; doi:10.3390/electronics7110288

Step 3: Determination of Fitness Function

The voltage/current parameters corresponding to BLDC motor are appeared in the moth evaluation.To store the fitness values of moth and flames OA_M and OB matrix are employed.

$$OA_M = \begin{bmatrix} OA_1 \\ OA_2 \\ \vdots \\ OA_n \end{bmatrix} = \begin{Bmatrix} f\left[(A_{1,1}\ A_{1,2}\ \ldots\ A_{1,m})\right] \\ f\left[(A_{2,1}\ A_{2,2}\ \ldots\ A_{2,m})\right] \\ \vdots \\ f\left[(A_{n,1}\ A_{n,2}\ \ldots\ A_{n,m})\right] \end{Bmatrix} \qquad (14)$$

$$OB = \begin{bmatrix} OB_1 \\ OB_2 \\ \vdots \\ OB_n \end{bmatrix} = \begin{Bmatrix} f\left[(b_{1,1}\ b_{1,2}\ \ldots b_{1,m})\right] \\ f\left[(b_{2,1}\ b_{2,2}\ \ldots b_{2,m})\right] \\ \vdots \\ f\left[(b_{n,1}\ b_{n,2}\ \ldots b_{n,m})\right] \end{Bmatrix} \qquad (15)$$

The main objective of the activation function of the proposed algorithm is to minimize error generated from reference and measured signal. Also, The $f_i(t)$ can be expressed mathematically as, $f_i(t) = \min\{V_e\}$ where, V_e is the error signal.

Step 4: Position Updating

The each moth position is updated based on the best fitness value and is expressed in equation (16). Here, t is the random number, d is distance and S is spiral function.

$$S(A_i, B_J) = d_i . e^{bt} . \cos(2\pi t) + B_j \qquad (16)$$

Where, $d_i = \left| B_j - A_i \right|$

During spatial orientation, no moths should cross upper limit and when moth becomes closer to flame, preceding parameters should be updated with respect to current parameters. The random number t is in interval [r, 1] and iteration process r decreases with linear relation from -1 to -2.

Step 5: Final Process

The adaptive mechanism employed in number of flames over the iterations as follows,

$$flame\_no = round(N_{\max} - 1 * \frac{N_{\max} - 1}{T_{\max}}) \qquad (17)$$

Peer-reviewed version available at *Electronics* **2018**, *7*, 288; doi:10.3390/electronics7110288

Where, $T_{\max}$ and $N_{\max}$ represents the maximal flames number and iteration. Positions of moths have been updated by considering best flame from end iterations which provides adjustments of gradually minimization of investigated and searched position. These fulfilled datasets are given to the fuzzy logic controller to perform and predicts the most ideal control signals of the converter.The flowchart of proposed MFO algorithm with FLC is delineated in the Figure 4.

3.2. Prediction of Control Signals Using FLC

The FLC algorithm is utilized to perform and predicts the most ideal control signals of the converter.The procedure of FLC is indicated underneath. FLC controller makes results encourage decisively by improved interest and MFFLC strategy is utilized for power factor correction with parameters gain.

(i) *Fuzzification Process:* With the help of membership function selection, it converts crisp to linguistic parameters [31,32]. The error $E\ (t)$ and the change of error $E_c(t)$ are considered as supply parameters of FLC which is given as,

$$E\ (t)=V_o(t)-V_{ref}(t) \qquad (18)$$

$$E_g(t)=E_p(t)-E_{p-1}(t) \qquad (19)$$

Where, the reference voltage is $V_{ref}(t)$, the present output voltage is $V_o(t)$, and p subscripts denotes the initial considered parameters.

(ii)*Fuzzy Inference Engine:* With the application of If-Then fuzzy rules, decisions are taken as:

$$If\ E\ \ is\ A_i\ \ and\ \ E_c\ is\ B_i,\ THEN\ Z_i^f(t)\ is\ f_i(t) \qquad (20)$$

Where, A_i, B_i and $f_i(t)$ are subsets and singleton parameters, respectively.

(iii)*De-Fuzzification Process:* In this method, fuzzy variables are defuzzified and converted to numerical output.It decides membership ability of output parameters.The outcome of the framework database as,

$$f_i(t)=Z_i^f(t) \qquad (21)$$

Where, $Z_i^f(t)$ is represents the solution of target after fuzzification.

This segment deals MFFLC strategy performance with VSI controlled BLDCM which are implemented using MATLAB/Simulink platform. At first, the parameters likes peed, torque, stator current, back EMF and torque ripple minimization of BLDC motor is examined. For creating the closed loop of BLDC motor the Cuk converter is utilized and optimal torque reference signal is generated based on speed controller. Meanwhile, to control BLDC motor the control signals are given to DC-DC converter by PWM generator from voltage based controller. In view of above procedure, the simulation is performed for various speed and torque conditions under three different test cases.

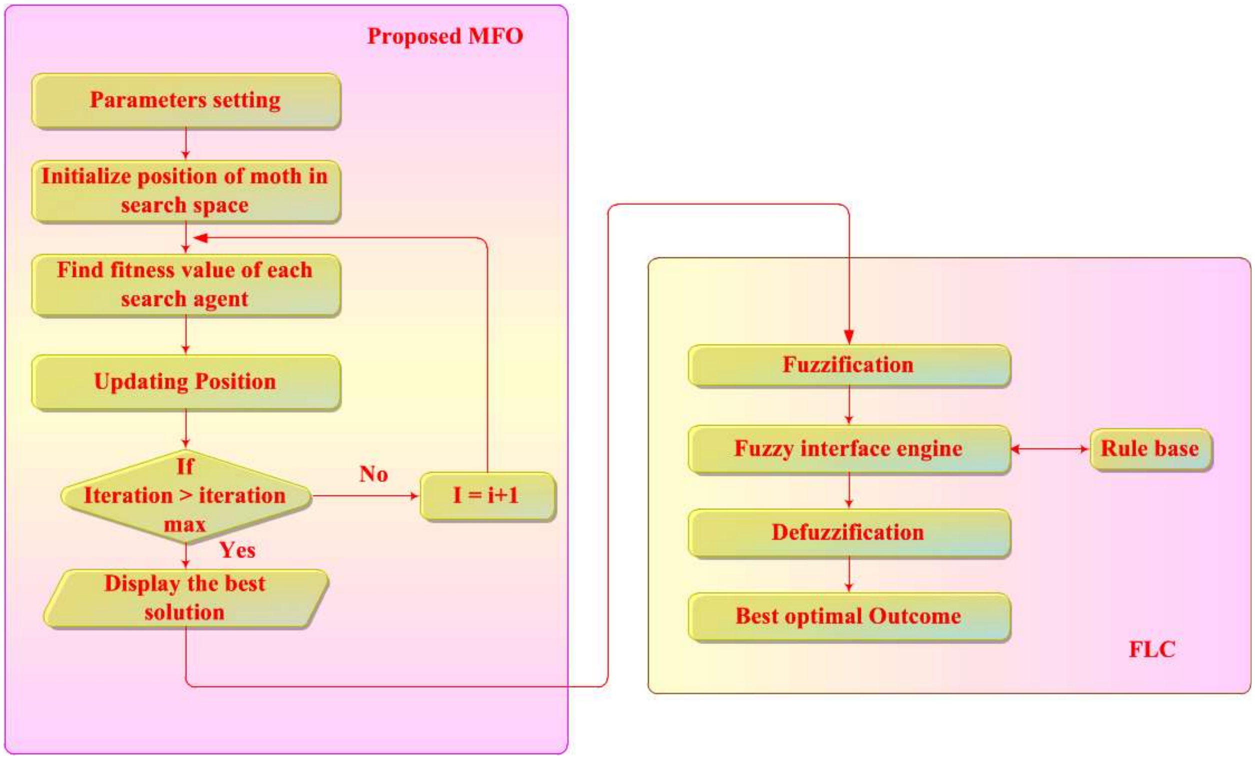

Figure 4. Flow chart of proposed MFFLC method

4. Simulated Results and Discussions

Test Case 1: Analysis of Constant Speed and Torque

In the sub section, the steady state performance of BLDCM has been discussed. For this steady state analysis of BLDC motorthe speed (1500 rpm)and torque (5 Nm) is fixed as constant. Here, by using the proposed methodologies, the optimized speed and torque in BLDC motor is controlled. Additionally, enhancements of existing techniques are MFO and PI controller, which is equated versus proposed method. The proposed tuning process has been tested under constant speed and torque, which is illustrated in the Figure 5 respectively. Here, the proposed method to reach the settling time is 0.25 seconds respectively. The existing methods are achieving the settling process at 0.27 seconds, 0.32 seconds respectively. The optimization methodology optimizes the current, speed, EMF and torque of the proposed technique based on the minimization of error produced from measured performance and reference output performance. The optimized tuning parameters from the proposed methodology assure that the best fit output system behaviour. Speed at constant speeds (1500rpm) to reach the settling time at 0.38 seconds is achieved using PI controller.

Preprints (www.preprints.org) | NOT PEER-REVIEWED | Posted: 24 September 2018 doi:10.20944/preprints201809.0462.v1

Peer-reviewed version available at *Electronics* **2018**, *7*, 288; doi:10.3390/electronics7110288

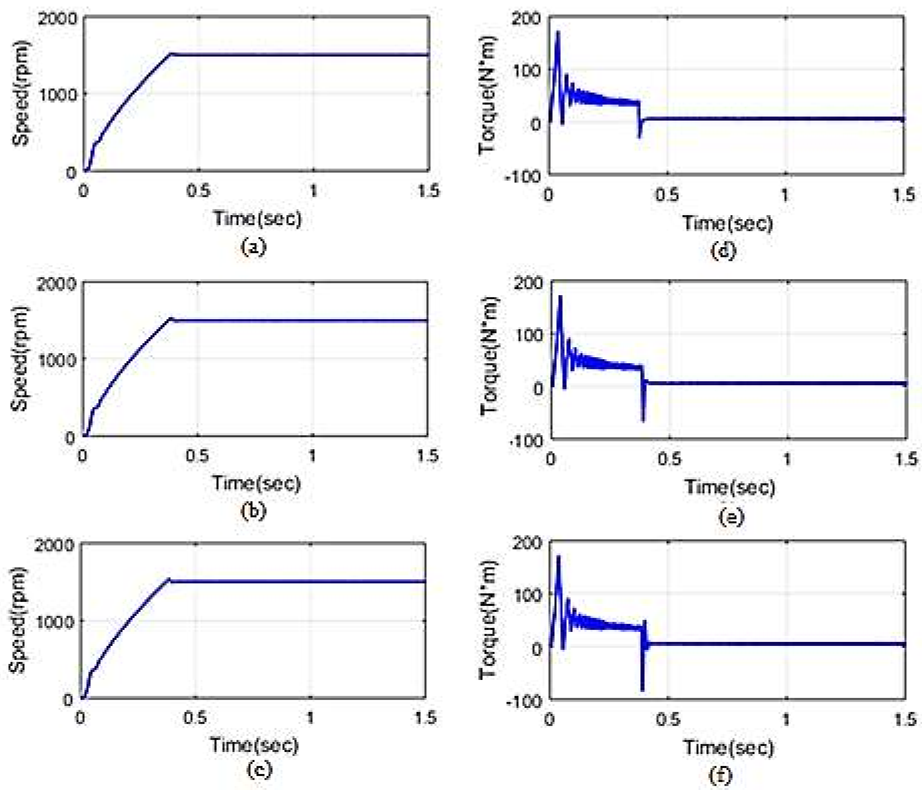

Figure 5. Analysis of Speedusing the(a) proposed (b) MFOmethod and (c) PI controller and Torque using the(d) proposed (e) MFOmethod and (f) PI controller

Figure 6 shows the analysis of capacitor and inductor, current and voltage using proposed method. The Figure 6(a-c) shows, the behaviour of proposed drives used inductors and capacitors components for correction of power factor which result improvement of power quality and can be achieved by the complete range of speed control. Figure 6 (d), 6 (e) shows the different operation of switch with optimal voltage/current. By increasing time, DC-link voltage is increases and reached maximum of 387 V, thereby corrected the power it can be seen in Figure 6(f).

The output performance analysis of EMF and PWM with proposed and existing methodologies is described in the Figure 7. In the figure, the output performance of the BLDC motor, the proposed method has rise time at 0 speeds (rpm) and takes 1.02 seconds to achieve the stable condition. In Figure 7 (b) show that, MFO methodology gets the speed at constant speeds (rpm) rise time and settling process at 0.4 seconds. The PI controller speed process requires 0.41 seconds to settling process. Similarly, the dynamic states are analyzed in the following section. In Figure 7 (d), when the switch is ON, the pulse is generated at the time interval of 1 to 1.00007 sec and in existing method the pulses are generated in between the time interval of 1.00007sec to 1.00011sec is illustrated in Figure 7 (e) and (f).

Preprints (www.preprints.org) | NOT PEER-REVIEWED | Posted: 24 September 2018 doi:10.20944/preprints201809.0462.v1

Peer-reviewed version available at Electronics 2018, 7, 288; doi:10.3390/electronics7110288

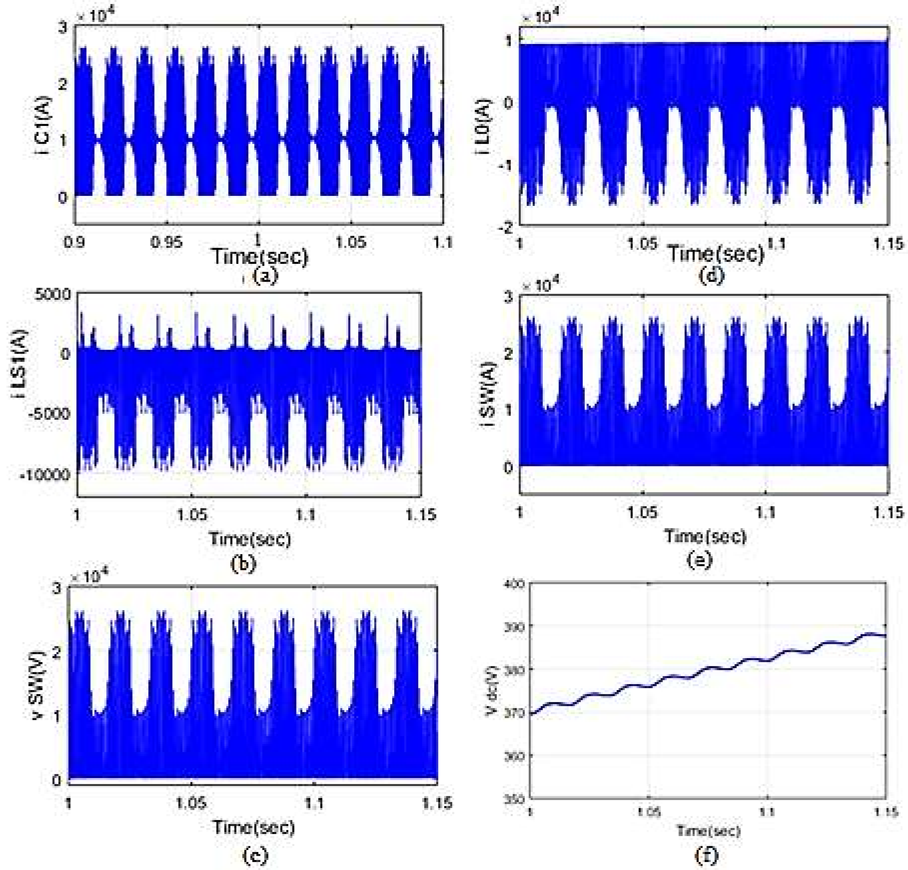

Figure 6. Analysis of current using the (a) C_1, (b) L_1, (d) L_0, (e) switch and voltage using (c) switch, (f) DC link

Test Case 2: Analysis of Constant Torque with Speed Variation

In this segment, the torque is constant and speed is varied and the proposed method based BLDC motor effectiveness is simulated with the different methods such as, MFO method, and the PI controller. Based on the motor regulated speed and torque, the torque ripple is minimized. The motor speed is controlled in view of input parameters of BLDC motor like current and back electromotive force. Comparison between speed and time of the proposed, MFO and PI controller simulation is illustrated in Figure 8.In Figure 8 (a) shows the motor initially starts at a speed of 0 rpm and gradually increases to 1500 rpm by stepped period of 0.38 s and 0.4 to 1 sec of the settling period. After that the speed of motor decreased to 900 rpm. In Figure 8 (b) shows that the motor initially starts at a speed of 0 rpm and gradually increases a speed by stepped period of 0.37 sec and settling period is 0.37 to 1 sec. After that the speed of motor decreased to 900 rpm in the MFO technique. In Figure 8 (c) shows that the motor initially starts at a speed of 0 rpm and gradually increases a speed by stepped period of 0.35 sand 0.35 to 1 sec of settling period in PI controller. After that the speed of motor decreased to 900 rpm. The comparison between Torque and time of the proposed, MFO and PI controller simulation is illustrated in figure 8. In Figure 8 (d) shows the motor torque is kept at constant. But the time will be varies 0 to 0.42 sec in proposed method. In Figure 8 (e) shows that the time variation in the motor in MFO method is 0 to 0.38 sec due to the constant torque

Preprints (www.preprints.org) | NOT PEER-REVIEWED | Posted: 24 September 2018 doi:10.20944/preprints201809.0462.v1

Peer-reviewed version available at *Electronics* **2018**, *7*, 288; doi:10.3390/electronics7110288

condition. In Figure 8 (f) shows that the time variation in the motor in PI controller is 0 to 0.37 sec due to the constant torque condition.

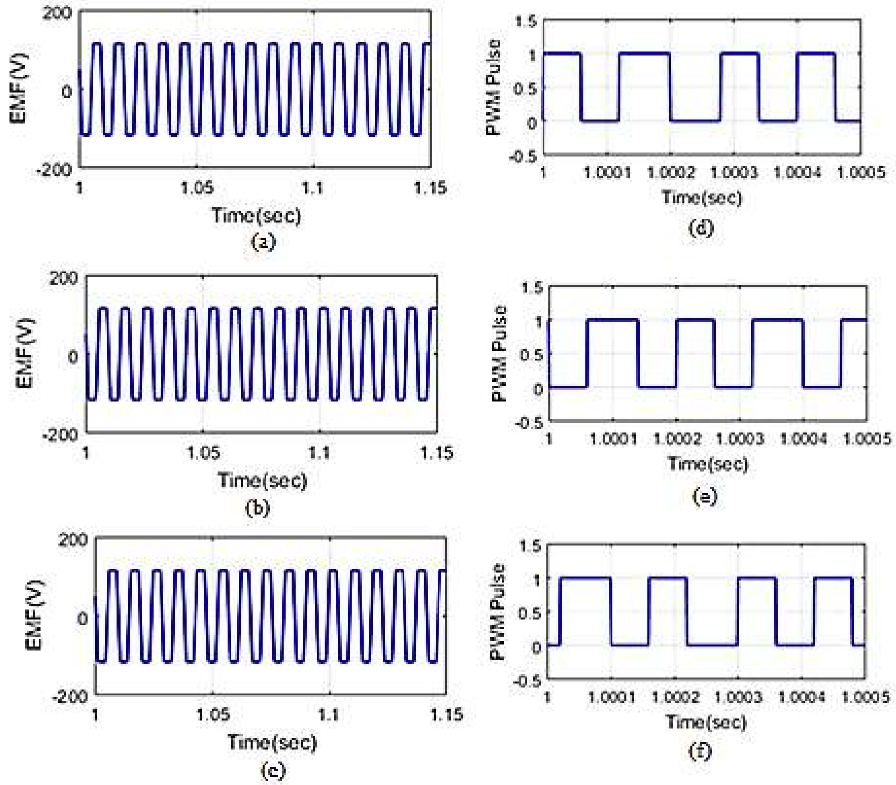

Figure 7. Analysis of EMF using the (a) proposed (b) MFO method and (c) PI controllerand PWM using the (d) proposed (e) MFOmethod and (f) PI controller

Figure 9 shows the analysis of capacitor and inductor, current and voltage using proposed method. Figure 9 (a-c) shows the performance of proposed drive system operates using supply/ output inductor /capacitor for power factor correction. The power quality improvement has been realized by the entire range of speed control. Figure 9 (d), (e) illustrates the different modes of switch working with optimal voltage/current stress. By increment in time period, DC-link voltage is increases and reached maximum of 383 V with a time interval of 0.9 to 1.1sec.

The comparison between EMF and time of the proposed, MFO and PI controller simulation has been described using figure 10. It explains the EMF of the proposed technique start run at normally. The value of the EMF value ranges from 1.2 to 1.6 sec. In Figure 10 (b) shows the EMF of the MFO technique start run at normally. The value of the EMF value ranges from 1.1 to 1.6 sec. In Figure 10c shows the EMF of the PI controller start run at normally. The value of the EMF value ranges from 0.9 to 1.6 sec. The comparison between PWM signals and time of the proposed, MFO and PI controller simulation is illustrated in Figure 10. Comparing the proposed technique with existing technique, the proposed

Peer-reviewed version available at *Electronics* **2018**, *7*, 288; doi:10.3390/electronics7110288

technique generate PWM generates full pulse. But in the existing technique, the PWM generate half the pulse in the proposed technique.

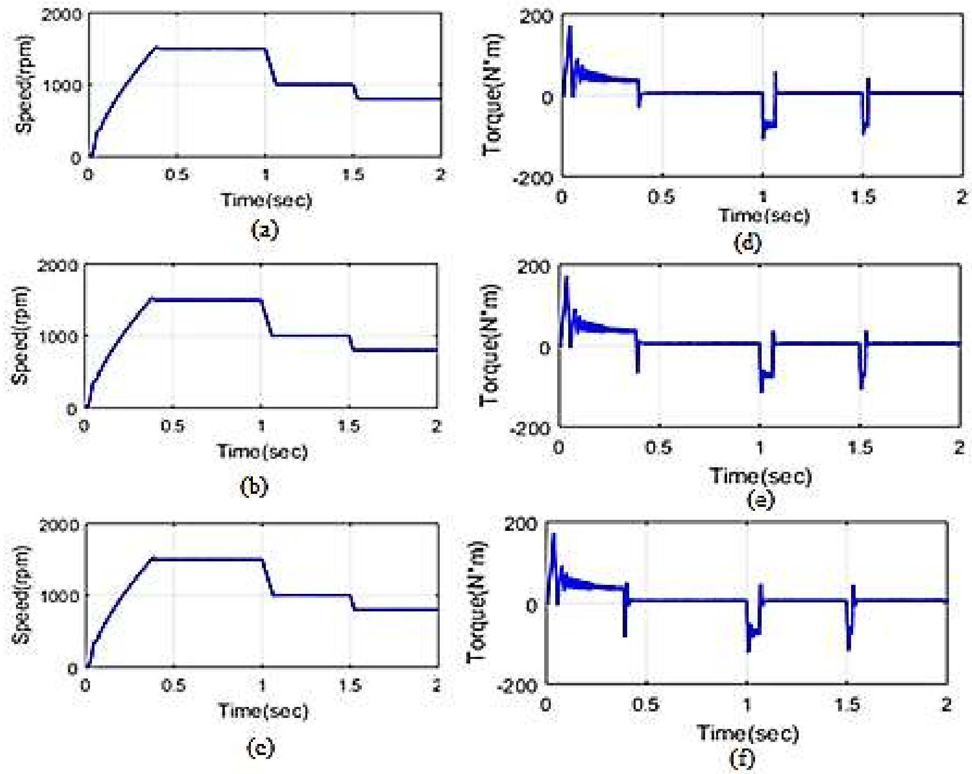

Figure 8. Analysis of Speedusing the (a) proposed (b) MFOmethod and (c) PI controllerand Torque using the (d) proposed (e) MFOmethod and (f) PI controller

Test Case 3: Analysis of Torque Variation with Constant Speed

This section describes about the performance analysis of proposed method based on the minimization of BLDCM torque distortion. The employed strategy is utilized to achieve the power factor control of BLDC motor. The output performance by using the proposed methodologies and other methods are desribed in Figure 11. While comparing the proposed methods takes constant rise time with speed ranges from 0 to 0.4 sec in 1500 rpm i.e.., the speed is constant. The MFO method based speed process takes from 0 to 0.42sec and it needed constant seconds to stabilize the system in Figure 11 (b) and in PI controller the speed process is not constant appeared in 11 (c). But the proposed method describes the nature of braking torque which increases as none zero current for any step. Figure 11 shows that, the analysis of torque is varied in every 0.45 sec with employed and classical methodologies have been illustrated. The behaviour of speed output of employed controller contains constant rise and settling time of 1500 (rpm) seconds.

Preprints (www.preprints.org) | NOT PEER-REVIEWED | Posted: 24 September 2018 doi:10.20944/preprints201809.0462.v1

Peer-reviewed version available at Electronics 2018, 7, 288; doi:10.3390/electronics7110288

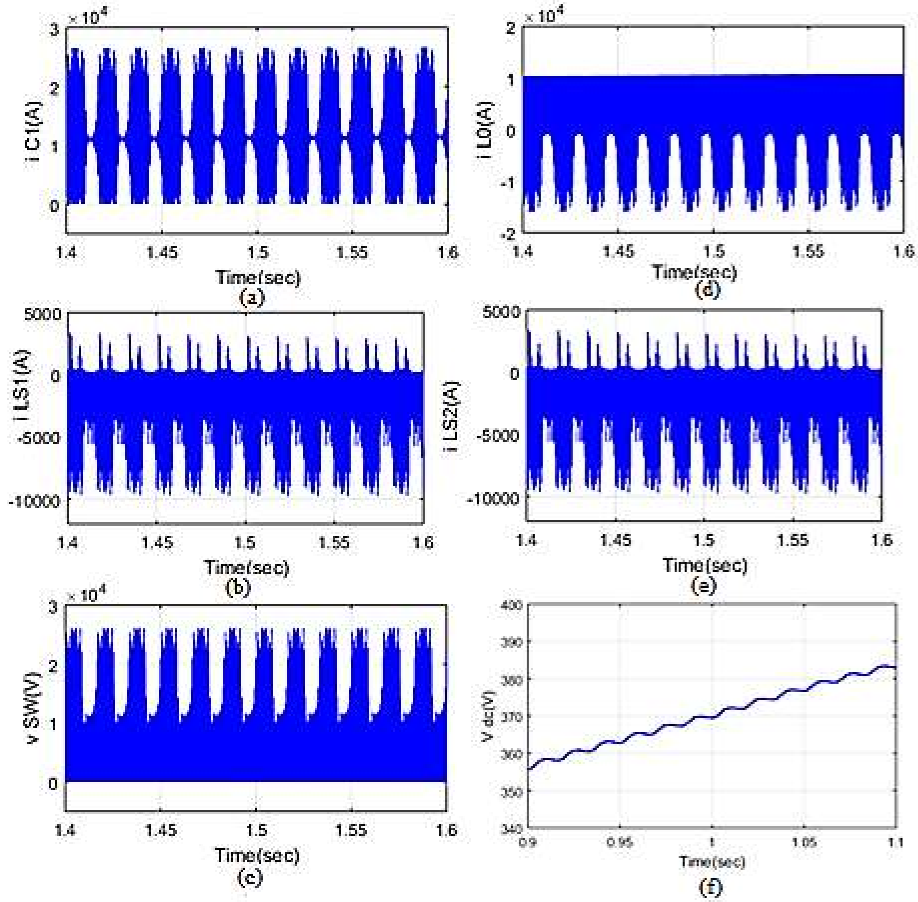

Figure 9. Analysis of current using the (a) C_1, (b) L_1, (d) L_0, (e) switch and voltage using (c) switch, (f) DC link

Figure 12 shows the analysis of capacitor and inductor, current and voltage using proposed method. Fig 12 (a-c) (i) shows the steady state behaviour of proposed drive system which operates using supply inductor and capacitor with output inductor and capacitor for power factor correction. The enhanced quality of power can be obtained by entire speed adjustment range. Different mode of operation of switch with optimal voltage/ current stress has been explained using Figure 12 (d, e). By increment of time period, DC-link voltage increases and reached maximum of 381 V with a time interval of 0.9 to 1.1s.

In Figure 13 shows the BLDC motor is optimized as the EMFanalysis for the proposed method, MFO, PI controller operation. In Figure 13, EMF of the proposed method and other techniques time are varied for settling process. Here, the proposed method takes the less time settling process with compare to the existing methods like as MFO and PI controller. The analysis of EMF and PWM output performance of the proposed and existing methods has been illustrated in the Figure13 respectively.

In proposed, the pulse is generated within the seconds when the switch is ON condition and in existing the pulse is generated (rising) from zero and fall at t=1.00021 sec.Figure 14 and table 1 shows the power factor correction of BLDC motor with three different test cases. While comparing with existing method, the proposed MFFLC method has power factor of 0.777 in test case 1, 0.767 in test case 2, and 0.742 in test

Peer-reviewed version available at Electronics 2018, 7, 288; doi:10.3390/electronics7110288

case 3.Hence,by utilizing the proposed strategy the PFC is identified and there is a decrement in ripple torque by half amount in BLDC motor by different speed and torque variation. On the other hand, the existing methods have analyzed to reduce the torque ripples and provide the superiority over the existing methods having more complex computational analysis. Thus, proposed control system enhances the stability and accurateness of drive scheme and reduces complex computation performance by correcting and adding supplementary components associated to conventional approaches.

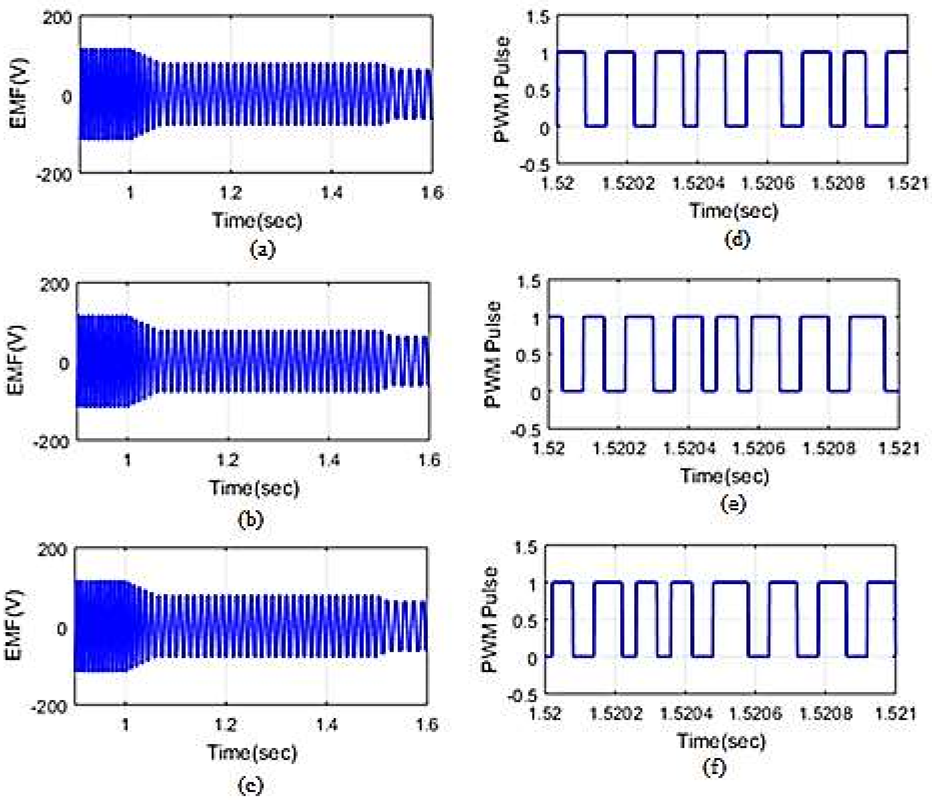

Figure 10. Analysis of EMF using the (a) proposed (b) MFOmethod and (c) PI controllerand PWM using the (d) proposed (e) MFOmethod and (f) PI controller

Table 1. Power factor of BLDC motor with proposed technique

Methods	**Power factor**		
	Case 1	**Case 2**	**Case 3**
Proposed	0.9772	0.9675	0.9428
MFO	0.9542	0.9402	0.9156
PI controller	0.9435	0.9292	0.8921

Peer-reviewed version available at Electronics 2018, 7, 288; doi:10.3390/electronics7110288

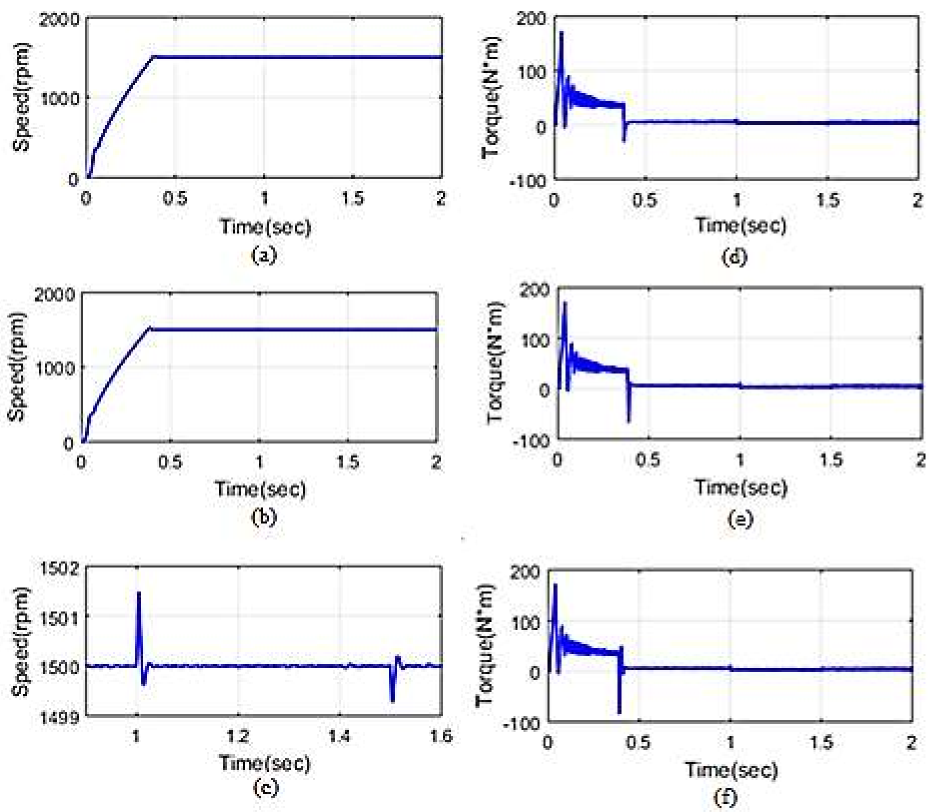

Figure 11. Analysis of Speed using the (a) proposed (b) MFOmethod and (c) PI controllerand Torque using the (d) proposed (e) MFOmethod and (f) PI controller

5. Conclusion

In this paper, the MFFLC strategy was utilized for analyzing the dynamic behaviour of BLDC motor. The proposed strategy based BLDC motor was actualized in MATLAB/Simulink stage. Here, the modelling and controlling process are done by using the proposed technique. In the modelling part, the BLDC motor was fed through the DBR, DC filter, enhanced PFC based Cuk converter and VSI devices. In the controlling part, the voltage and current is controlled utilizing the proposed control strategy. Thus, an enhanced PI controller is presented for PFC at ac supply, and reducing torque ripple of BLDCM. It was tested with three different test cases of speed and torque conditions. In these conditions, the actual speed, rated speed, torque, current, back EMF, PFC and the minimization of ripple in torque of BLDC motor is dissected. Proposed controller has been executed by taking account of present controllers such as MFO method and PI controller. Additionally, the generation of PWM signals minimize the torque ripples. The viability of employed methods have been discussed with suitable rise/settling periods. From the performance analysis, the suggested method shows better execution over that of the current strategies.

Preprints (www.preprints.org) | NOT PEER-REVIEWED | Posted: 24 September 2018 doi:10.20944/preprints201809.0462.v1

Peer-reviewed version available at Electronics 2018, 7, 288; doi:10.3390/electronics7110288

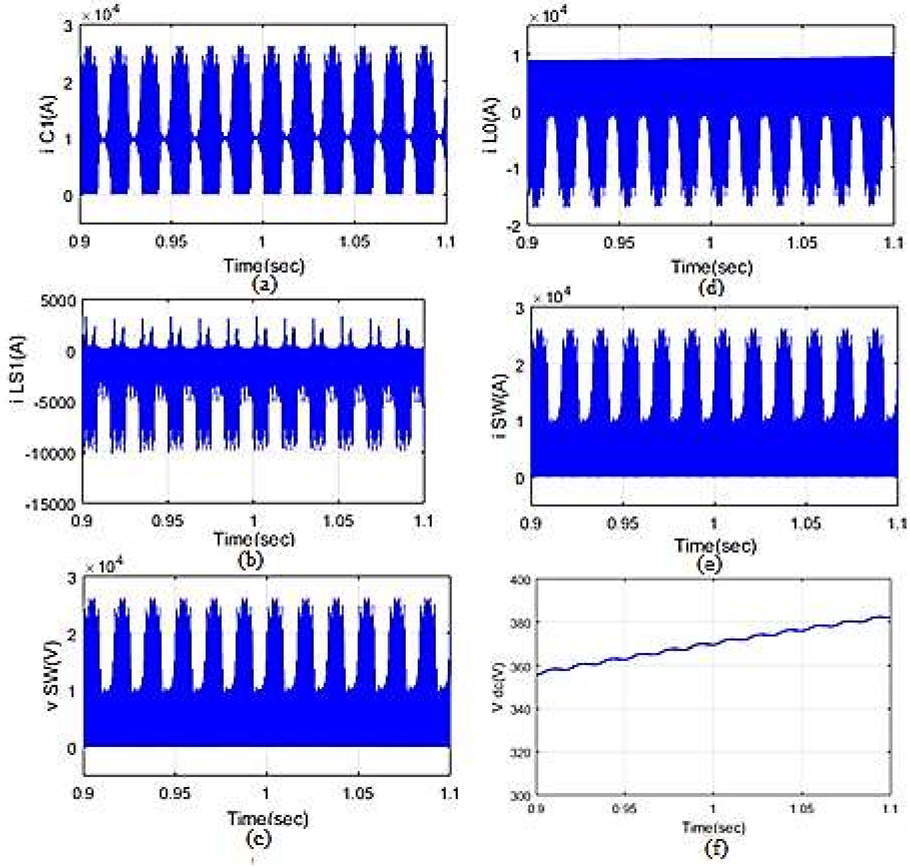

Figure 12. Analysis of current using the (a) C_1, (b) L_1, (d) L_0, (e) switch and voltage using (c) switch, (f) DC link

Preprints (www.preprints.org) | NOT PEER-REVIEWED | Posted: 24 September 2018 doi:10.20944/preprints201809.0462.v1

Peer-reviewed version available at *Electronics* **2018**, *7*, 288; doi:10.3390/electronics7110288

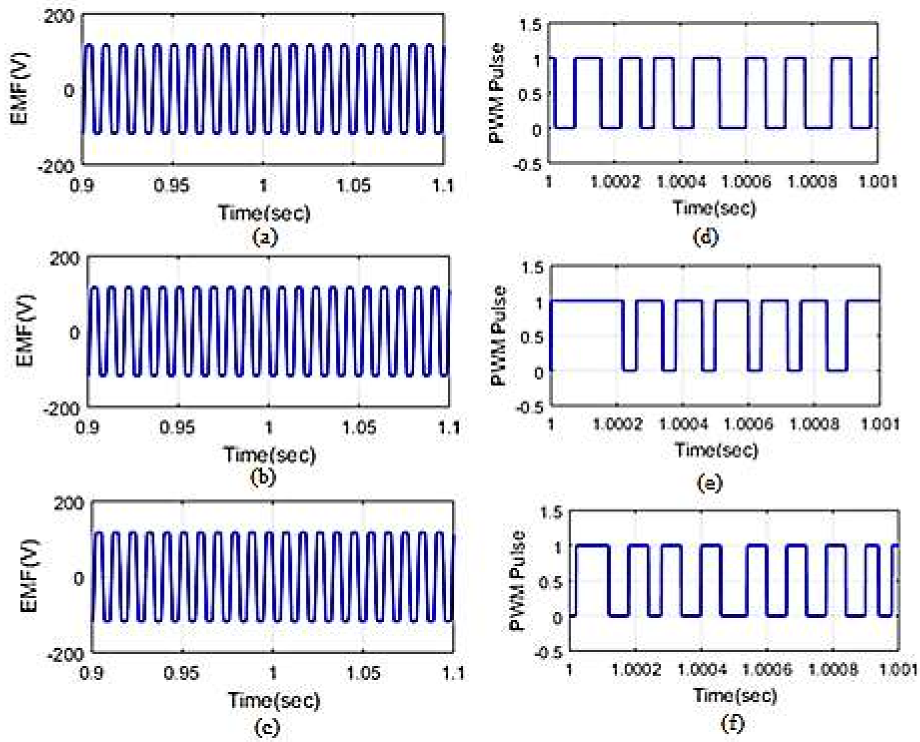

Figure 13. Analysis of EMF using the (a) proposed (b) MFOmethod and (c) PI controllerand PWM using the (d) proposed (e) MFOmethod and (f) PI controller

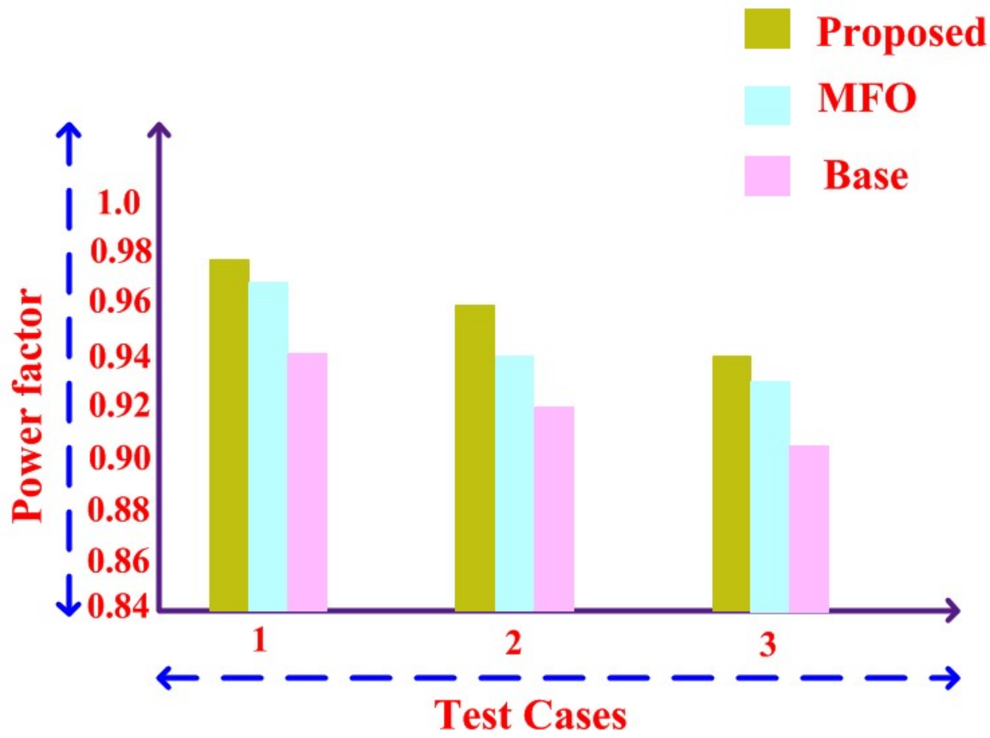

Figure 14. Performancecomparison of power factor with different test cases

 doi:10.20944/preprints201809.0462.v1

Peer-reviewed version available at *Electronics* **2018**, *7*, 288; doi:10.3390/electronics7110288

References

1. Priyadarshi, N.; Padmanaban, S.; Mihet-Popa, L.; Blaabjerg, F.; Azam, F. Maximum Power Point Tracking for Brushless DC Motor-Driven Photovoltaic Pumping Systems Using a Hybrid ANFIS-FLOWER Pollination Optimization Algorithm. *Energies***2018**, *11*, 1–16.
2. Ibrahim, H.E.A.; Hassan, F.N.;Shomer, A.O.; Optimal PID control of a brushless DC motor using PSO and BF techniques.*Ain Shams Engg. J.***2014**, 5, 371-398.
3. Niapour, S.A.KH.M.;Tabarraie, M.;Feyzi, M.R. A new robust speed-sensor less control strategy for high-performance brushless DC motor drives with reduced torque ripple. *Control Engg. Practice*. **2014**, 24, 42–54.
4. Masmoudi, M.;Badsi,B.E1.;Masmoudi, A. Direct Torque Control of Brushless DC Motor Drives with Improved Reliability.*IEEE Trans. on Ind. Appl*. **2014**, 50, 3744-3753.
5. Sheng, T.; Wang, X.; Zhang, J.; Deng, Z. Torque Ripple Mitigation for Brushless DC Machine Drive Systems Using One-Cycle Average Torque Control.*IEEE Trans. on Ind. Elec*. **2015**, 62, 2114-2122.
6. Lu, H.; Zhang, L.;Qu, W. A New Torque Control Method for Torque Ripple Minimization of BLDC Motors With Un-Ideal Back EMF. *IEEE Trans. on Power Elec.***2008**, 23, 750-758.
7. Tingna, S.;Yuntao, G.;Peng, S.;Changlian, C. A new approach of minimizing commutation torque ripple for brushless DC motor based on DC–DC converter. IEEE Trans. on Ind. Elec.**2010**, 57, 3483-3470.
8. Jiancheng, F.;Xinxiu, Z.; Gang, L. Precise Accelerated Torque Control for Small Inductance Brushless DC Motor.*IEEE Trans. on Power Elec*. **2013**, 28, 1400-1412.
9. Devendra, P.; Chandra, K.P.B.; Arasaratnam, I.; Gu, -D.W.; Mary, K.A.; CH,S.B. Derivative-free square-root cubature Kalman filter for non-linear brushless DC motors.*IET Electric Power Appl.***2016**, 10, 417-427.
10. Jiancheng, F.;Xinxiu, Z.; Gang, L. Instantaneous Torque Control of Small Inductance Brushless DC Motor.*IEEE Trans. on Power Elec*. **2012**, 27, 4952-4964.
11. Devendra, P.;Kalyan,Ch.P.; Mary, K.A.; Ch.S.B. Simulation Approach for Torque Ripple Minimization of BLDC Motor Using Direct Torque Control.*Int. J. of Adv. Research in Elec., Electronics and Instrum.Engg.***2013**, 3703-3710.
12. Shanmugasundram, R.;Zakariah, K.M;Yadaiah, N. Implementation and Performance Analysis of Digital Controllers for Brushless DC Motor Drives. *IEEE/ASME Trans. on Mechatronics.***2014**,213-224.
13. Jiancheng, F.;Xinxiu, Z.; Gang, L. Instantaneous Torque Control of Small Inductance Brushless DC Motor. *IEEE Trans. on Power Elec.***2012**, 27, 4952-4964 .
14. Tingna, S.; Yuntao, G.; Peng, S.; Changlian, C. A new approach of minimizing commutation torque ripple for brushless DC motor based on DC–DC converter.*IEEE Trans. on Ind. Elec.* **2010**, 57, 3483-3470.
15. Sathyan, A.; Milivojevic, N.; Lee, -Y.J.; Krishnamurthy, M.;Emadi, A. An FPGA-Based Novel Digital PWM Control Scheme for BLDC Motor Drives. *IEEE Trans. on Ind. Elec*. **2007**,56, 3040-3047.
16. Lee, -B.K.; Kim, T.H.;Ehsani, M. On the feasibility of four-switch three-phase BLDC motor drives for low cost commercial applications: topology and control.*IEEE Trans. on Power Elec.***2003**, 18,164-172.
17. Park, S.J.; Park, H.W.; Lee, M.H.;Harashima, F. A new approach for minimum-torque-ripple maximum-efficiency control of BLDC motor. *IEEE Trans. on Ind. Elec*. **2000**, 47, 107-114.
18. Liu, Y.; Zhu, Z.Q.; Howe, H. Direct Torque Control of Brushless DC Drives With Reduced Torque Ripple. *IEEE Trans. on Ind. Appl*. **2005**, 41, 577-608.
19. Wang, Y.; Chau, K.T.; Chan, C.C.; Jiang, J.Z. Transient Analysis of a New Outer-Rotor Permanent-Magnet Brushless DC Drive Using Circuit-Field-Torque Coupled Time-Stepping Finite-Element Method.*IEEE Trans. on Magnetics*. **2002**, 38, 1277-1300.
20. Chau, K.T.; Chan, C.C.; Liu, C. Overview of Permanent-Magnet Brushless Drives for Electric and Hybrid Electric Vehicles. *IEEE Trans. on Ind. Elec*. **2008**, 55, 2246-2257.

21. Priyadarshi, N.; Padmanaban, S.; Maroti, P.K.; Sharma, A. An Extensive Practical Investigation of FPSO-Based MPPT for Grid Integrated PV System Under Variable Operating Conditions with Anti-Islanding Protection. *IEEE Syst. J.***2018**, *PP*. 1–11.
22. Pandey, R.; Singh, B. Improved power quality SEPIC converter fed series resonant inverter for induction heater. In Proc. of 1st Int. Conf. on Power Elec., Intel. Control and Energy Sys. (ICPEICES). 2016, pp.1-6.
23. Foroozeshfar, R.; Farzanehfard, H.;Adib, E. New single-stage, single-switch, soft-switching three-phase SEPIC and Cuk-type power factor correction converters.*IET Power Elec*. **2014**, 1878-1885.
24. Poorali, B.;Adib, E.;Farzanehfard, H. Soft-switching DC–DC Cuk converter operating in discontinuous-capacitor-voltage mode.*IET Power Elec.***2017**, 10, 1677-1686.
25. Buso, S.; Spiazzi, G.;Tagliavia, D. Simplified control technique for high-power-factor flybackCuk and Sepic rectifiers operating in CCM.*IEEE Trans. on Ind. Appl*. **2000**, 36,1413-1418.
26. Jiang, G.; Xia, C.; Chen, W.; Tingna, S.; Li, X.; Cao, Y.Commutation Torque Ripple Suppression Strategy for Brushless DC Motors with a Novel Non-inductive Boost Front End.*IEEE Trans. on Power Elec*.**2017**, 33, 4274-4284.
27. Nasirian, V.;Karimi, Y.;Davoudi, A.;Zolghadri, M.; Ahmadian, M.;Moayedi, S. Dynamic Model Development and Variable Switching-Frequency Control for DCVM Cúk Converters in PFC Applications.*IEEE Trans. on Ind. Appl*. **2013**, 47, 2636-2650.
28. Mirjalili, S. Moth-flame optimization algorithm: A novel nature-inspired heuristic paradigm. *Knowledge-Based Systems*. **2015**, 87, 228-249.
29. Gaston, K.; Bennie, J.; Davies, T.; Hopkins, J. The ecological impacts of nighttime light pollution: a mechanistic appraisal.*Biological Reviews*. **2013**, 88, 712-727.
30. Langevelde, F.V.;Ettema, J.;Donners, M.;WallisDeVries, M.;Groenendijk, D. Effect of spectral composition of artificial light on the attraction of moths. *Biological Conservation*. **2011**, 144, 2274-2281.
31. Ali, J.A.;Hannan, M.A.; Mohamed, A.;Abdolrasol, M.G. Fuzzy logic speed controller optimization approach for induction motor drive using backtracking search algorithm.*ElsevierMeasurement*. **2016**,78,49-62.
32. Priyadarshi, N.; Padmanaban, S.; Bhaskar, M.S.; Blaabjerg, F.; Sharma, A. A Fuzzy SVPWM Based Inverter Control Realization of Grid Integrated PV-Wind System with FPSO MPPT Algorithm for a Grid-Connected PV/Wind Power Generation System: Hardware Implementation. *IET Electr. Power Appl*. **2018**, 12, 7, pp. 962–971